

Comparison of Different Theory Models and Basis Sets in the Calculations of Structures and ^{13}C NMR Spectra of [Pt(en)(CBDCA–O, O')], an Analogue of the Antitumor Drug Carboplatin

Hongwei Gao,* Xiujuan Wei, Xuting Liu, and Tingxia Yan

Institute of Watershed Science and Environmental Ecology, Wenzhou Medical College, Zhejiang, 325035, China

Received: December 19, 2009; Revised Manuscript Received: February 11, 2010

Comparisons of various density functional theory (DFT) methods at different basis sets in predicting the molecular structures and ^{13}C NMR spectra for [Pt(en)(CBDCA–O, O')], an analogue of the antitumor drug carboplatin, are reported. DFT methods including B3LYP, B3PW91, mPW1PW91, PBE1PBE, BPV86, PBEPBE, and LSDA are examined. Different basis sets including LANL2DZ, SDD, LANL2MB, CEP-4G, CEP-31G, and CEP-121G are also considered. It is remarkable that the LSDA/SDD level is clearly superior to all of the remaining density functional methods in predicting the structure of [Pt(en)(CBDCA–O, O')]. The results also indicate that the B3LYP/SDD level is the best to predict ^{13}C NMR spectra for [Pt(en)(CBDCA–O, O')] among all DFT methods.

1. Introduction

Platinum complexes play an important role in the chemotherapy of various malignancies.^{1–5} The first generation of platinum drug is *cis*-diamminedichloroplatinum(II), *cis*-[PtCl₂(NH₃)₂] (clinically known as cisplatin),⁶ which was discovered in the 60s. Cisplatin is one of the first anticancer drugs that entered clinical treatment and which has lived an unreached story of success in the treatment of cancer. The second generation Pt drug carboplatin, [*cis*-diammine(1,1-cyclobutane-dicarboxylato)-platinum(II)] was developed in the 1980s. Carboplatin is the most widely used platinum drug for the treatment of cancer because it is much less nephrotoxic and neurotoxic than cisplatin.^{7,8} The slower hydrolysis of the cyclobutanedicarboxylate (CBDCA) leaving group in carboplatin reduces its toxicity in comparison to the chloride ligands in cisplatin.⁹

To improve the anticancer activity of platinum drugs, many research workers have made a lot of efforts. Over 3000 cisplatin analogues¹⁰ and other platinum(II) and platinum(IV) complexes have been prepared and tested against various types of tumors.^{11–14} Numerous theoretical and experimental investigations on the molecular properties and the mechanism of action for carboplatin and its analogue have been reported.^{15–20}

Giese et al.¹⁵ reported a tentative assignment of the vibration spectra of carboplatin. Wysokinski et al.¹⁶ provided the clear-cut assignment of the experimental infrared and Raman spectra of carboplatin at the mPW1PW91/LANL2DZ level. Tornaghi et al.¹⁷ calculated the structure of carboplatin and concluded that the six-membered chelate ring containing the dicarboxylate group has a boat conformation. The structure of carboplatin was also calculated by Adamo et al.¹⁸ and they reported that the B3LYP functional overestimates the Pt–N atom distances in carboplatin. Guo et al.¹⁹ reported the X-ray crystallographic and solid-state NMR spectra for [Pt(en)(CBDCA–O, O')].

So far, no attempt has been made to analyze the application of various DFT methods and different basis sets for accurate

calculations of structure and ^{13}C NMR spectra of large platinum(II) complexes.

The first purpose of this work is to investigate the performance of different DFT methods in predicting geometry and ^{13}C NMR spectra of [Pt(en)(CBDCA–O, O')]. The second purpose of this work is to study the effect of basis sets in predicting geometry and ^{13}C NMR spectra of [Pt(en)(CBDCA–O, O')]. This study provided a wealth of theoretical data giving insights into the kinetic and structural behavior of [Pt(en)(CBDCA–O, O')]-DNA complexes. A fundamental understanding of the properties of [Pt(en)(CBDCA–O, O')] is believed to be essential for the development of the antitumor drug and improvement for the platinum drug design.

2. Calculations

All the calculations have been carried out using the *Gaussian* 98 set of programs.²⁰ The properties and ^{13}C NMR spectra of [Pt(en)(CBDCA–O, O')] were determined through the application of various density functional theory (DFT) including B3LYP, B3PW91, MPW1PW91,²¹ PBE1PBE,²² BPV86, PBEPBE,²³ and LSDA²⁴ functional and different basis sets including LANL2DZ, SDD, LANL2MB, CEP-4G, CEP-31G, and CEP-121G. The calculated ^{13}C NMR spectra using *Gaussian* 98 are picked up by the *GaussView* 4.1 package.

^{13}C NMR spectra of [Pt(en)(CBDCA–O, O')] were calculated using the gauge-including atomic orbital method (GIAO).^{25–27} The NMR shielding for the carbon atoms of [Pt(en)(CBDCA–O, O')] were obtained with geometries optimized at the same theoretical levels.¹³ C NMR Isotropic Chemical Shieldings are referred to tetramethylsilane (TMS) calculated at the same theoretical levels.

3. Results and Discussion

3.1. Geometry Optimization with Various Methods at LANL2DZ Basis Set. The major problem with DFT calculation is that the exact functionals for exchange and correlation are not known except for the free electron gas. However, approximations in DFT permit the calculation of certain physical

* To whom correspondence should be addressed. Tel.: 0577-86699661, E-mail: gaohongw369@hotmail.com

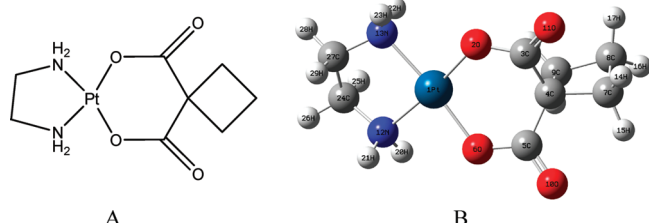


Figure 1. Molecular cluster model of $[\text{Pt}(\text{en})(\text{CBDCA}-\text{O}, \text{O}')]$: (A) The chemical structure; (B) The optimized structure at LSDA/LANL2DZ level.

quantities quite accurately. The most widely used approximation is the local-density approximation (LDA) in physics. The local spin-density approximation (LSDA) is a straightforward generalization of the LDA to include electron spin. The exchange energy in DFT hybrid methods (B3LYP, B3PW91, mPW1PW91, PBE1PBE, BPV86, PBEPBE, and LSDA methods at LANL2DZ

PBE1PBE1) is combined with the exact energy from Hartree–Fock theory. The adjustable parameters in hybrid functionals are generally fitted to a training set of molecules. Unfortunately, although the results obtained with these functionals are usually sufficiently accurate for most applications, there is no systematic way of improving them in contrast to some of the traditional wave function-based methods like configuration interaction or coupled cluster theory. Hence, it is necessary to estimate the error of the calculations for structure and properties of $[\text{Pt}(\text{en})(\text{CBDCA}-\text{O}, \text{O}')]$ comparing them to other methods or experiments.

The chemical structure (A) and optimized structure of $[\text{Pt}(\text{en})(\text{CBDCA}-\text{O}, \text{O}')]$ at LSDA/LANL2DZ level (B) are depicted in Figure 1. The optimized structures of $[\text{Pt}(\text{en})(\text{CBDCA}-\text{O}, \text{O}')]$ using HF, B3LYP, B3PW91, mPW1PW91, PBE1PBE, BPV86, PBEPBE, and LSDA methods at LANL2DZ

TABLE 1: Comparison of Bond Lengths (in Å) and Bond Angles (in Deg) Calculated with Various DFT Methods at LANL2DZ Basis Set for the Molecular Cluster Model of $[\text{Pt}(\text{en})(\text{CBDCA}-\text{O}, \text{O}')]$

geometry	exptl ^a	HF	B3LYP	B3PW91	mPW1PW91	PBE1PBE	BPV86	PBEPBE	LSDA
LANL2DZ									
R(C4–C7)	1.548	1.552	1.561	1.555	1.552	1.551	1.566	1.563	1.539
R(C7–C8)	1.538	1.555	1.564	1.559	1.556	1.555	1.569	1.566	1.549
R(C8–C9)	1.533	1.554	1.563	1.557	1.555	1.554	1.568	1.565	1.548
R(C4–C9)	1.543	1.582	1.596	1.588	1.584	1.583	1.602	1.598	1.575
R(C4–C5)	1.522	1.543	1.541	1.537	1.532	1.531	1.544	1.541	1.516
R(C5–O10)	1.232	1.223	1.247	1.244	1.242	1.242	1.258	1.258	1.246
R(C5–O6)	1.285	1.329	1.359	1.354	1.350	1.350	1.372	1.371	1.351
R(Pt1–O6)	2.017	1.987	2.007	1.998	1.990	1.990	2.018	2.018	1.980
R(Pt1–N12)	2.023	2.110	2.099	2.083	2.075	2.073	2.094	2.092	2.042
R(N12–C24)	1.480	1.493	1.509	1.500	1.499	1.498	1.516	1.513	1.491
R(C24–C27)	1.540	1.534	1.541	1.536	1.533	1.532	1.544	1.542	1.523
mean absolute deviation	0.026	0.032	0.030	0.073	0.024	0.024	0.035	0.033	0.016
$\angle(\text{C9–C4–C7})$	90.8	88.5	88.4	88.4	88.5	88.4	88.4	88.3	88.5
$\angle(\text{C8–C7–C4})$	88.7	89.9	90.0	89.9	89.8	89.8	90.0	89.9	89.6
$\angle(\text{O10–C5–C4})$	122.3	121.0	121.8	121.9	121.8	121.8	122.4	122.4	122.1
$\angle(\text{O10–C5–O6})$	119.0	121.6	120.1	120.3	120.4	120.5	119.5	119.6	120.4
$\angle(\text{N12–Pt1–O6})$	92.2	91.9	90.1	89.8	89.8	89.7	89.8	89.8	88.6
$\angle(\text{Pt1–N12–C24})$	106.6	108.5	108.3	108.1	108.1	108.0	108.2	108.1	107.6
$\angle(\text{N12–C24–C27})$	105.0	109.4	109.3	109.1	109.1	109.1	109.1	109.1	108.8

^a Experimental values are from ref 19.

TABLE 2: Comparison of Bond Lengths (in Å) and Bond Angles (in Deg) Calculated with LSDA Method at Different Basis Sets for the Molecular Cluster Model of $[\text{Pt}(\text{en})(\text{CBDCA}-\text{O}, \text{O}')]$

geometry	exptl ^a	LSDA				
		LANL2DZ	SDD	LANL2MB	CEP-31G	CEP-121G
R(C4–C7)	1.548	1.539	1.539	1.556	1.562	1.559
R(C7–C8)	1.538	1.549	1.548	1.555	1.571	1.565
R(C8–C9)	1.533	1.548	1.547	1.559	1.570	1.565
R(C4–C9)	1.543	1.575	1.575	1.579	1.597	1.595
R(C4–C5)	1.522	1.516	1.516	1.558	1.539	1.534
R(C5–O10)	1.232	1.246	1.245	1.255	1.265	1.262
R(C5–O6)	1.285	1.351	1.351	1.392	1.371	1.368
R(Pt1–O6)	2.017	1.980	1.977	1.960	1.989	1.989
R(Pt1–N12)	2.023	2.042	2.041	2.105	2.042	2.040
R(N12–C24)	1.480	1.491	1.491	1.510	1.511	1.507
R(C24–C27)	1.540	1.523	1.522	1.535	1.543	1.536
mean absolute deviation	0.016	0.021	0.038	0.032	0.029	
$\angle(\text{C9–C4–C7})$	90.8	88.5	88.4	89.4	88.5	88.4
$\angle(\text{C8–C7–C4})$	88.7	89.6	89.5	90.5	89.4	89.4
$\angle(\text{O10–C5–C4})$	122.3	122.1	122.1	123.7	122.2	122.0
$\angle(\text{O10–C5–O6})$	119.0	120.4	120.4	119.1	120.0	120.0
$\angle(\text{N12–Pt1–O6})$	92.2	88.6	88.9	91.5	88.1	88.2
$\angle(\text{Pt1–N12–C24})$	106.6	107.6	107.6	109.2	107.6	107.5
$\angle(\text{N12–C24–C27})$	105.0	108.8	108.8	108.2	108.4	108.5

^a Experimental values are from ref 19.

TABLE 3: Calculated ^{13}C NMR Isotropic Chemical Shieldings Using Various DFT Methods at LANL2DZ Basis Set and Corresponding Experimental Values for the Molecular Cluster Models of $[\text{Pt}(\text{en})(\text{CBDCA}-\text{O}, \text{O}')]$ (in ppm)

	exptl ^a	HHFF	B3LYP	B3PW91	mPW1PW91	PBE1PBE	BPV86	PBEPBE	LSDA
LANL2DZ									
C8	16.0	18.25	21.02	20.05	20.12	22.94	19.62	24.81	19.26
C7	31.7	26.46	33.34	31.63	31.47	34.34	32.40	37.61	33.72
C9		36.11	46.43	44.13	43.73	46.87	46.36	51.73	48.73
C27	48.7	43.50	48.73	47.69	47.70	50.68	47.47	52.87	49.02
C24	48.7	43.55	48.84	47.79	47.80	50.77	47.61	53.01	49.16
C4	56.9	58.13	63.86	62.07	62.21	65.17	61.79	67.11	64.85
C5	182.3	210.74	189.37	187.53	189.32	192.13	179.54	185.02	184.67
C3	182.3	211.03	189.56	187.70	189.44	192.18	179.71	185.06	184.71
(TMS ^b)	205.37	193.13	194.97	196.47	200.05	190.27	196.18	193.76	
Mean absolute deviation	9.53	3.51	2.73	3.21	5.20	2.11	4.86		2.34

^a Experimental values are from ref 19. ^b TMS: tetramethylsilane (reference).

TABLE 4: Calculated ^{13}C NMR Isotropic Chemical Shieldings Using B3LYP Methods at Various Basis Sets and Corresponding Experimental Values for the Molecular Cluster Models of $[\text{Pt}(\text{en})(\text{CBDCA}-\text{O}, \text{O}')]$ (in ppm)

	exptl ^a	LANL 2DZ	SDD	LANL2MB	CEP-31G	CEP-121G
C8	16.0	19.26	17.73	46.75	27.97	26.23
C7	31.7	33.72	31.89	52.79	52.61	45.87
C9		48.73	47.97	55.20	49.38	48.06
C27	48.7	49.02	47.52	73.05	57.14	49.80
C24	48.7	49.16	47.75	73.05	57.79	50.48
C4	56.9	64.85	62.90	72.02	35.23	59.55
C5	182.3	184.67	182.62	144.84	179.01	175.25
C3	182.3	184.71	182.50	144.74	181.82	177.14
reference (TMS ^b)		193.76	191.04	250.41	-2.91	5.37
mean deviation		2.34	1.32	23.83	9.48	5.26

^a Experimental values are from ref 19. ^b TMS: tetramethylsilane.

basis set are similar to ones of $[\text{Pt}(\text{en})(\text{CBDCA}-\text{O}, \text{O}')]$ calculated at LSDA/LANL2DZ level.

The calculated geometrical parameters with various DFT methods at LANL2DZ basis set are listed in Table 1. For comparison, the experimental results from X-ray crystal analysis of $[\text{Pt}(\text{en})(\text{CBDCA}-\text{O}, \text{O}')]$ are also listed in Table 1.¹⁹

In Table 1, we have compared the results obtained from various DFT calculations using LANL2DZ basis set with experimental results. It is seen that the Pt1–N12 bond distances yielded by the B3LYP, B3PW91, mPW1PW91, PBE1PBE, BPV86, and PBEPBE methods are significantly overestimated, whereas that calculated with the LSDA protocol (2.042 Å) is nearest to the experimental data. Furthermore, LSDA predicts the C7–C8 (1.549 Å), C8–C9 (1.548 Å), C4–C9 (1.575 Å), C4–C5 (1.516 Å), and N12–C24 (1.491 Å) lengths in better agreement with experiment than all other methods.

To investigate the performance and limits of the different DFT methods in predicting the bond length of $[\text{Pt}(\text{en})(\text{CBDCA}-\text{O}, \text{O}')]$, the mean absolute deviations between the calculated values and experimental ones for each method are also given in Table 1.

The mean absolute deviations between the calculated bond length and experimental value are 0.026 Å for HF, 0.032 Å for B3LYP, 0.030 Å for B3PW91, 0.073 Å for mPW1PW91, 0.024 Å for PBE1PBE, 0.035 Å for BPV86, 0.033 Å for PBEPBE, and 0.016 Å for LSDA, respectively. These results indicate that LSDA method is the best choice to predict the bond length of $[\text{Pt}(\text{en})(\text{CBDCA}-\text{O}, \text{O}')]$.

The calculated N12–C24–C27 angles of $[\text{Pt}(\text{en})(\text{CBDCA}-\text{O}, \text{O}')]$ with various DFT methods at LANL2DZ basis set are larger than experimental value by about 3–5°. The calculated other angles including C9–C4–C7, C8–C7–C4, O10–C5–C4, O10–C5–C6, and Pt1–N12–C24 for $[\text{Pt}(\text{en})(\text{CBDCA}-\text{O}, \text{O}')]$ with various DFT methods at LANL2DZ basis set for the molecular cluster model of $[\text{Pt}(\text{en})(\text{CBDCA})]$ are shown in Figure 2.

($\text{CBDCA}-\text{O}, \text{O}'$) with various DFT methods at LANL2DZ basis set are very close to the experimental values.

3.2. Geometry Optimization with LSDA Methods at Various Basis Sets. We have investigated the effects of the basis sets on the geometry of $[\text{Pt}(\text{en})(\text{CBDCA}-\text{O}, \text{O}')]$ by using LSDA methods at various basis sets. A comparison of the calculated geometry parameters for $[\text{Pt}(\text{en})(\text{CBDCA}-\text{O}, \text{O}')]$ with LSDA methods at different basis sets is presented in Table 2.

The mean absolute deviations between the calculated bond length and experimental value are 0.016 Å for LANL2DZ, 0.021 Å for SDD, 0.038 Å for LANL2MB, 0.032 Å for CEP-31G, and 0.029 Å for CEP-121G, respectively. These results indicate that LANL2DZ and SDD basis sets are the best choice to predict the bond length of $[\text{Pt}(\text{en})(\text{CBDCA}-\text{O}, \text{O}')]$.

The calculated N12–C24–C27 and N12–Pt1–O6 angles of $[\text{Pt}(\text{en})(\text{CBDCA}-\text{O}, \text{O}')]$ with the LSDA method at various basis sets are larger than experimental value by about 3–4°. The calculated other angles including C9–C4–C7, C8–C7–C4, O10–C5–C4, O10–C5–C6, and Pt1–N12–C24 for $[\text{Pt}(\text{en})(\text{CBDCA}-\text{O}, \text{O}')]$ with various DFT methods at LANL2DZ basis set are very close to the experimental values.

3.3. NMR Spectra Calculated with Various Methods at the LANL2DZ Basis Set. Calculated ^{13}C NMR isotropic chemical shieldings using various DFT methods at the LANL2DZ basis set and corresponding experimental values for the molecular cluster model of $[\text{Pt}(\text{en})(\text{CBDCA})]$ (in ppm) are given in Table 3. Calculated ^{13}C NMR spectra using various DFT methods at LANL2DZ basis set for the molecular cluster model of $[\text{Pt}(\text{en})(\text{CBDCA})]$ are shown in Figure 2.

Five signals can be observed in the $^{13}\text{C}\{\text{H}\}$ NMR solution spectrum of $[\text{Pt}(\text{en})(\text{CBDCA})]$ at 298 K.¹⁹ In this literature, five signals were assigned to the ring carbons C8 (16.0 ppm), C7

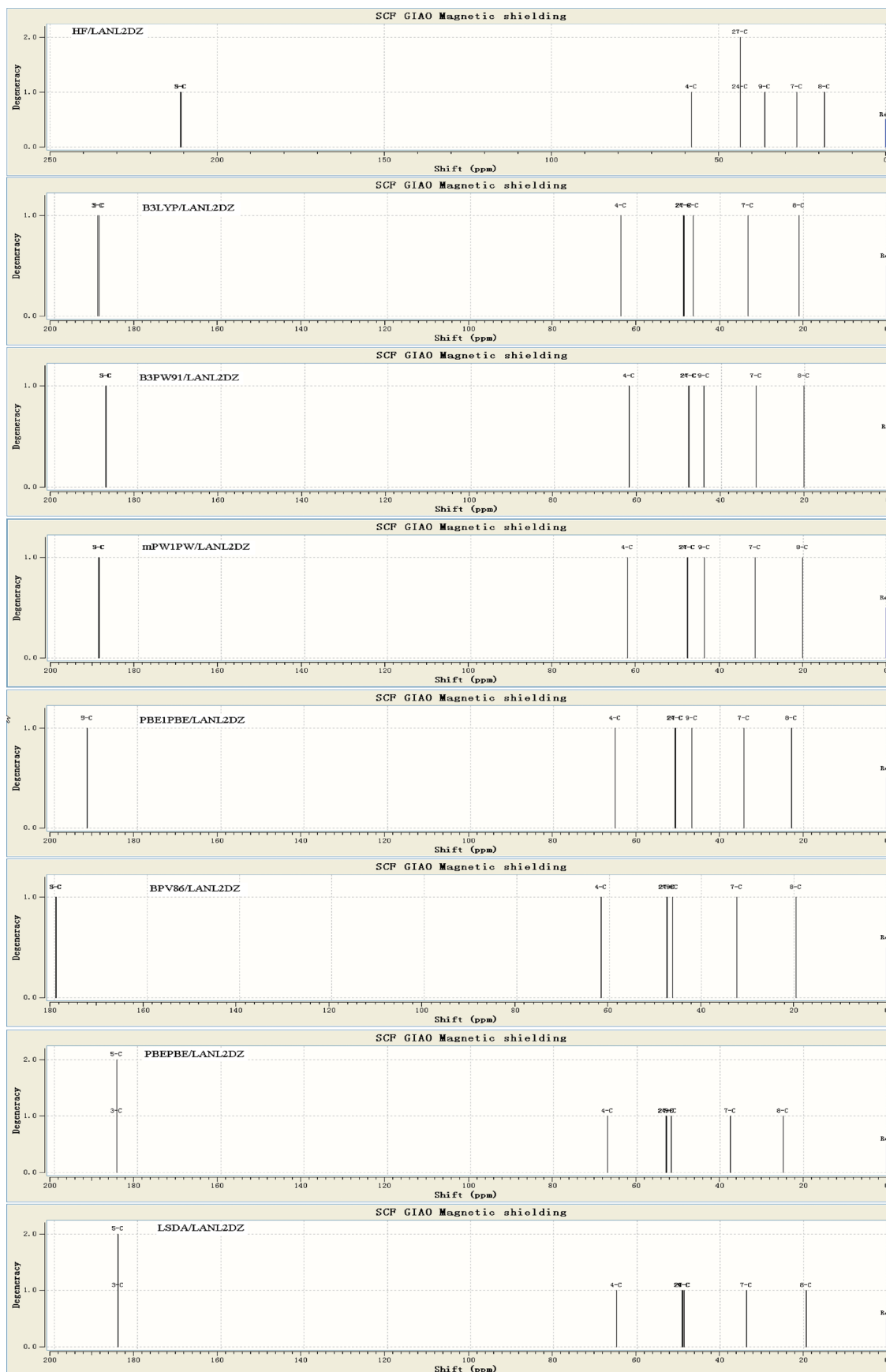


Figure 2. Calculated ¹³C NMR isotropic chemical shieldings using various DFT methods at LANL2DZ basis set for [Pt(en)(CBDCA-O, O')].

and C9 (31.7 ppm), C4 (56.9 ppm), the carboxyl carbons C3 and C5 (182.3 ppm) of CBDCA, and the methylene carbons

C24 and C27 (48.7 ppm) of ethylenediamine. Similar ¹³C NMR spectra for [Pt(en)(CBDCA)] have been calculated in Figure 2.

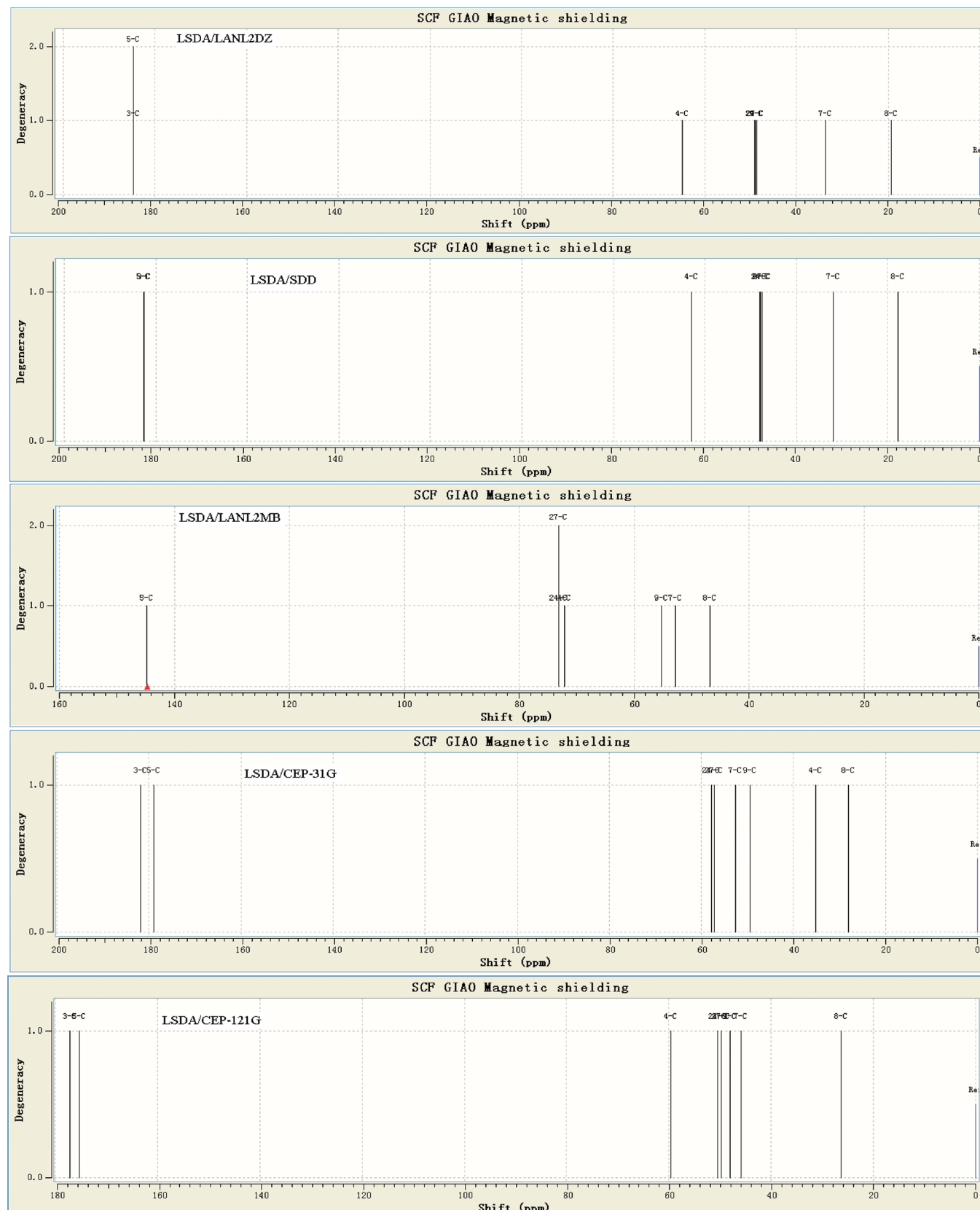


Figure 3. Calculated ^{13}C NMR isotropic chemical shieldings using LSDA method at various basis sets for $[\text{Pt}(\text{en})(\text{CBDCA}-\text{O}, \text{O}')]$.

To investigate the performance and limits of different DFT methods in predicting the ^{13}C NMR spectra, the mean absolute deviation between the calculated ^{13}C NMR isotropic chemical shieldings and experimental values for $[\text{Pt}(\text{en})(\text{CBDCA})]$ are also given in Table 3.

The mean absolute deviation between the calculated ^{13}C NMR isotropic chemical shieldings and experimental values for $[\text{Pt}(\text{en})(\text{CBDCA})]$ are 19.87 ppm for HF, 6.63 ppm for B3LYP, 9.03 ppm for B3PW91, 10.13 ppm for mPW1PW91, 10.79 ppm for PBE1PBE, 7.80 ppm for BPV86, 8.24 ppm for PBEPBE,

and 8.56 ppm for LSDA, respectively. As we can see, HF method is insufficient for reliable predictions of ¹³C NMR spectra for [Pt(en)(CBDCA)], whereas the DFT-based methods that include a significant fraction of electron correlation can give reliable results for predicting ¹³C NMR spectra for [Pt(en)(CBDCA)]. The calculated results indicate that B3LYP method is the best choice for studying ¹³C NMR spectra for [Pt(en)(CBDCA)].

The calculation results show that the crystal structure of [Pt(en)(CBDCA—O, O')] is best described by the LSDA functional in all DFT methods, the crystal structure determines the properties of materials, therefore, the LSDA functional performed better in NMR calculation than the other seven DFT methods.

The electronic structure of [Pt(en)(CBDCA—O, O')] is better described by the LSDA functional than the improvement of GGA and meta-GGA functionals, maybe this is main reason why the improvement of GGA and meta-GGA functionals give worse prediction of NMR spectra.

3.4. Vibrational Spectra Calculated with PBE1PBE Methods at Various Basis Sets. Calculated ¹³C NMR isotropic chemical shieldings using LSDA methods at various basis sets and corresponding experimental values for the molecular cluster model of [Pt(en)(CBDCA)] (in ppm) are listed in Table 4. Calculated ¹³C NMR spectra for [Pt(en)(CBDCA)] using LSDA methods at various basis sets are shown in Figure 3.

The calculated ¹³C NMR isotropic chemical shieldings for C7 in [Pt(en)(CBDCA)] with LSDA methods at LANL2DZ, SDD, LANL2MB, CEP-31G, and CEP-121G basis sets are 33.72, 31.89, 52.79, 52.61, and 45.87 Å respectively in Table 4. In comparison with the same experimental value of 31.7 ppm,²⁰ overestimation of experimental frequency values is about 6.37% for LANL2DZ, 0.59% for SDD, 66.52% for LANL2MB, 65.96% for CEP-31G, and 44.7% for CEP-121G basis sets. The calculated ¹³C NMR isotropic chemical shieldings for C7 in [Pt(en)(CBDCA)] with LSDA method at SDD basis set show best agreement with experimental value. The results for C7 in [Pt(en)(CBDCA)] with LSDA method at LANL2DZ basis set also show good agreement with experimental value. The calculated ¹³C NMR isotropic chemical shieldings for other C atoms in [Pt(en)(CBDCA)] with LSDA methods at various basis sets have similar results.

The mean absolute deviation between the calculated ¹³C NMR isotropic chemical shieldings and experimental values for [Pt(en)(CBDCA)] are 2.34 ppm for LANL2DZ, 1.32 ppm for SDD, 23.83 ppm for LANL2MB, 9.48 ppm for CEP-31G, and 5.26 ppm for CEP-121G, respectively. The calculated results indicate that LANL2DZ and SDD basis sets are the best choice for studying ¹³C NMR spectra of [Pt(en)(CBDCA)].

The observed chemical shift in the zero-pressure limit is determined not only by the value of the shielding at the equilibrium geometry but also by the dynamic average over the multidimensional shielding surface during rotation and vibration of the molecule. In the gas, solution, or adsorbed phase, it is an average of the intermolecular shielding surface over all of the configurations of the molecule with its neighbors. Quantum mechanical descriptions of electronic structure and theories related to dynamics averaging of any electronic property can be subjected to stringent test.²⁸ The size of the basis set have a great influence on the calculation of chemical shift, and similar work can be found in the literature.^{29–32}

4. Conclusions

The most important findings of this work are the following:

(1) It is remarkable that the LSDA/SDD and LSDA/LANL2DZ levels are clearly superior to all of the remaining DFT levels in predicting the structures of [Pt(en)(CBDCA)], an analogue of the antitumor drug carboplatin.

(2) DFT methods considered here showed good performance in ¹³C NMR spectra calculations and usually provided a better performance than the Hartree–Fock methods for [Pt(en)(CBDCA)]. In particular, LSDA/SDD and LSDA/LANL2DZ levels afforded the best quality to predict ¹³C NMR spectra for [Pt(en)(CBDCA)].

Acknowledgment. This work is supported by Zhejiang Provincial Natural Science Foundation (Y5080043), Scientific Research Foundation of Wenzhou Medical College (QTJ07014), and Wenzhou Municipal Science and Technology Bureau (H20090080).

References and Notes

- Raymond, E.; Faivre, S.; Chaney, S.; Woynarowski, J.; Cvitkovic, E. Cellular and Molecular Pharmacology of Oxaliplatin. *Mol. Cancer Ther.* **2002**, *1*, 227–235.
- Raymond, E.; Chaney, S. G.; Taamma, A.; Cvitkovic, E. Oxaliplatin: A review of preclinical and clinical studies. *Ann. Oncol.* **1998**, *9*, 1053–1071.
- Fuertes, M. A.; Castilla, J.; Alonso, C.; Perez, J. M. Cisplatin biochemical mechanism of action: From cytotoxicity to induction of cell death through interconnections between apoptotic and necrotic pathways. *Curr. Med. Chem.* **2003**, *10*, 257–266.
- Ong, S. T.; Vogelzang, N. J. Chemotherapy in malignant pleural mesothelioma. *Ann. Rev. J. Clin. Oncol.* **1996**, *14* (3), 1007–1017.
- Weiss, R. B.; Christian, M. C. New cisplatin analogues in development. *Drugs* **1993**, *46* (3), 360–377.
- (a) Rosenberg, B.; Van Camp, L.; Krigas, T. Inhibition of cell division in escherichia coli by electrolysis products from a platinum electrode. *Nature* **1965**, *205*, 698–699. (b) Rosenberg, B.; Van Camp, L.; Trosko, J. E.; Mansour, V. H. Platinum compound. A new class of potent antitumour agents. *Nature* **1969**, *222*, 385–386.
- Sandman, K. E.; Lippard, S. J. In *Cisplatin*; Lippert, B., Ed.; VHCA and Wiley-VCH: Weinheim, Germany, 1999.
- Barnard, C. F. J.; Raynaud, F. I.; Kelland, L. R. In *Metallopharmaceuticals I: DNA Interactions*; Clarke M.j., Sadler P. j., Eds.; Springer: Berlin, 1999.
- Van der Vijgh, W. J. F. Clinical pharmacology of carboplatin. *Clin. Pharmacokin.* **1991**, *21*, 242–261.
- Weiss, R. B.; Christian, M. C. New cisplatin analogues in development. A review. *Drugs* **1993**, *46* (3), 360–377.
- Basch, H.; Krauss, M.; Stevens, W. J.; Cohen, D. Electronic and geometric structures of Pt(NH₃)₂²⁺, Pt(NH₃)₂Cl₂, Pt(NH₃)₂X, and Pt(NH₃)₂XY (X, Y = H₂O, OH⁻). *Inorg. Chem.* **1985**, *24* (21), 3313–3317.
- Reedijk, J. Why does cisplatin reach guanine-N7 with competing S-donor ligands available in the cell. *Chem. Rev.* **1999**, *99*, 2499–2510.
- Lippert, B. Impact of cisplatin on the recent development of Pt coordination chemistry: A case study. *Coord. Chem. Rev.* **1999**, *182*, 263–295.
- Wong, E.; Giandomenico, C. M. Current status of platinum-based antitumor drugs. *Chem. Rev.* **1999**, *99*, 2451–2466.
- Giese, B.; Deacon, G. B.; Kuduk-Jaworska, J.; McNaughton, D. Density functional theory and surface enhanced Raman spectroscopy characterization of novel platinum drugs. *Biopolymers* **2002**, *67*, 294–297.
- Wysokinski, R.; Kuduk-Jaworska, J.; Michalska, D. Electronic structure, Raman and infrared spectra, and vibrational assignment of carboplatin. Density functional theory studies. *J. Mol. Struct. Theochem.* **2006**, *758*, 169–179.
- Tornaghi, E.; Andreoni, W.; Carloni, P.; Hutter, J.; Parrinello, M. Carboplatin versus cisplatin: Density functional approach to their molecular properties. *Chem. Phys. Lett.* **1995**, *246*, 469–474.
- Adamo, C.; Barone, V. Exchange functionals with improved long-range behavior and adiabatic connection methods without adjustable parameters: The mPW and mPW1PW models. *J. Chem. Phys.* **1998**, *108*, 664–675.
- Guo, Z. J.; Habtemariam, A.; Sadler, P. J.; Palmerb, R.; Potter, B. S. Conformational flexibility within the chelate rings of [Pt(en)(CBDCA—O, O')] - an analogue of the antitumor drug carboplatin: X-ray crystallographic and solid-state NMR studies. *New J. Chem.* **1998**, *11*–14.
- Frisch, M. J.; Trucks, G. W.; Schlegel, H. B.; Scuseria, G. E.; Robb, M. A.; Cheeseman, J. R.; Zakrzewski, V. G.; Montgomery, J. A.; Stratmann,

- R. E.; Burant, J. C.; Dapprich, S.; Millam, J. M.; Daniels, A. D.; Kudin, K. N.; Strain, M. C.; Farkas, O.; Tomasi, J.; Barone, V.; Cossi, M.; Cammi, R.; Mennucci, B.; Pomelli, C.; Adamo, C.; Clifford, S.; Ochterski, J.; Petersson, G. A.; Ayala, P. Y.; Cui, Q.; Morokuma, K.; Malick, D. K.; Rabuck, A. D.; Raghavachari, K.; Foresman, J. B.; Cioslowski, J.; Ortiz, J. V.; Baboul, A. G.; Stefanov, B. B.; Liu, G.; Liashenko, A.; Piskorz, P.; Komaromi, I.; Gomperts, R.; Martin, R. L.; Fox, D. T.; Keith, T.; Al-Laham, M. A.; Peng, C. Y.; Nanayakkara, A.; Gonzalez, C.; Challacombe, M.; Gill, P. M. W.; Johnson, G. B.; Chen, W.; Wong, W.; Andres, J. L.; Head-Gordon, M.; Replogle, E. S.; Pople, J. A. *Gaussian 98*; Gaussian Inc.: Pittsburgh, PA, 1998.
- (21) Adamo, C.; Barone, V. Exchange functionals with improved long-range behavior and adiabatic connection methods without adjustable parameters: The mPW and mPW1PW models. *J. Chem. Phys.* **1998**, *108*, 664–675.
- (22) Perdew, J. P.; Burke, K.; Ernzerhof, M. Generalized gradient approximation made simple. *Phys. Rev. Lett.* **1996**, *77*, 3865–3868.
- (23) Perdew, J. P.; Burke, K.; Ernzerhof, M. Generalized gradient approximation made simple [Phys. Rev. Lett. **1996**, *77*, 3865]. *Phys. Rev. Lett.* **1997**, *78*, 1396–1396.
- (24) Vosko, S. H.; Wilk, L.; Nusair, M. Accurate spin-dependent electron liquid correlation energies for local spin density calculations: A critical analysis. *Can. J. Phys.* **1980**, *58*, 1200–1211.
- (25) Ditchfield, R. Self consistent perturbation theory of diamagnetism. I. gauge invariant LCAO method for NMR chemical shifts. *Mol. Phys.* **1974**, *27*, 789–807.
- (26) Ditchfield, R. Theoretical studies of magnetic shielding in H_2O and $(\text{H}_2\text{O})_2$. *J. Chem. Phys.* **1976**, *65*, 3123–3129.
- (27) Ditchfield, R. GIAO studies of magnetic shielding in FHF- and HF. *Chem. Phys. Lett.* **1976**, *40*, 53–56.
- (28) Jameson, C. J. Understanding NMR chemical shifts. *Annu. Rev. Phys. Chem.* **1996**, *47*, 135–169.
- (29) Czajlik, A.; Perczel, A. Peptide models XXXII. Computed chemical shift analysis of penetratin fragments. *J. Mol. Struct. Theochem.* **2004**, *675* (1–3), 129–139.
- (30) Tormena, C. F.; Silva, G. V. J. Chemical shifts calculations on aromatic systems: A comparison of models and basis sets. *Chem. Phys. Lett.* **2004**, *398* (4–6), 466–470.
- (31) Hratchian, H. P.; Milletti, M. C. First principles determination of ^{99}Ru chemical shifts using moderately sized basis sets. *J. Mol. Struct. Theochem.* **2005**, *724* (1–3), 45–52.
- (32) Higashioji, T.; Hada, M.; Sugimoto, M.; Nakatsuji, H. Basis set dependence of magnetic shielding constant calculated by the Hartree–Fock/finite perturbation method. *Chem. Phys.* **1996**, *203* (2), 159–175.

JP912005A